Physics and Imaging in Radiation Oncology 28 (2023) 100488

Contents lists available at ScienceDirect

Physics and Imaging in Radiation Oncology

journal homepage: www.sciencedirect.com/journal/physics-and-imaging-in-radiation-oncology

Original Research Article

Selective sparing of bladder and rectum sub-regions in radiotherapy of prostate cancer combining knowledge-based automatic planning and multicriteria optimization

Lisa Alborghetti [a], Roberta Castriconi [a,*], Carlos Sosa Marrero [b], Alessia Tudda [a], Maria Giulia Ubeira-Gabellini [a], Sara Broggi [a], Javier Pascau [c], Lucia Cubero [c], Cesare Cozzarini [d], Renaud De Crevoisier [b], Tiziana Rancati [e], Oscar Acosta [b], Claudio Fiorino [a]

[a] IRCCS San Raffaele Scientific Institute, Medical Physics, Milano, Italy
[b] CLCC Eugène Marquis, INSERM, LTSI—UMR1099, F-35000, Univ Rennes, Rennes, France
[c] Universidad Carlos III de Madrid, Bioengineering Department, Madrid, Spain
[d] IRCCS San Raffaele Scientific Institute, Radiotherapy, Milano, Italy
[e] Fondazione IRCCS Istituto Nazionale dei Tumori (INT), Progetto Prostata, Milano, Italy

ARTICLE INFO

Keywords:
Prostate cancer
Radiotherapy
Automated planning
Dose-outcome correlation
Multi-criteria optimization

ABSTRACT

Background and Purpose: The association between dose to selected bladder and rectum symptom-related sub-regions (SRS) and late toxicity after prostate cancer radiotherapy has been evidenced by voxel-wise analyses. The aim of the current study was to explore the feasibility of combining knowledge-based (KB) and multi-criteria optimization (MCO) to spare SRSs without compromising planning target volume (PTV) dose delivery, including pelvic-node irradiation.

Materials and Methods: Forty-five previously treated patients (74.2 Gy/28fr) were selected and SRSs (in the bladder, associated with late dysuria/hematuria/retention; in the rectum, associated with bleeding) were generated using deformable registration. A KB model was used to obtain clinically suitable plans (KB-plan). KB-plans were further optimized using MCO, aiming to reduce dose to the SRSs while safeguarding target dose coverage, homogeneity and avoiding worsening dose volume histograms of the whole bladder, rectum and other organs at risk. The resulting MCO-generated plans were examined to identify the best-compromise plan (KB + MCO-plan).

Results: The mean SRS dose decreased in almost all patients for each SRS. D1% also decreased in the large majority, less frequently for dysuria/bleeding SRS. Mean differences were statistically significant ($p < 0.05$) and ranged between 1.3 and 2.2 Gy with maximum reduction of mean dose up to 3–5 Gy for the four SRSs. The better sparing of SRSs was obtained without compromising PTVs coverage.

Conclusions: Selectively sparing SRSs without compromising PTV coverage is feasible and has the potential to reduce toxicities in prostate cancer radiotherapy. Further investigation to better quantify the expected risk reduction of late toxicities is warranted.

1. Introduction

External-beam radiation therapy is one of the leading options in the curative treatment of prostate cancer. However, the presence of partial overlap between the bladder and the treatment target can lead to long-term urinary symptoms, which are considered significant challenges following prostate radiotherapy [1,2]. Besides, it is widely acknowledged that radiation-induced toxicity involves complex biological processes in the irradiated tissues and is not solely dependent on the delivered dose [3,4].

* Corresponding author.
E-mail addresses: alborghetti.lisa@hsr.it (L. Alborghetti), castriconi.roberta@hsr.it (R. Castriconi), carlos.sosa@univ-rennes.fr (C. Sosa Marrero), tudda.alessia@hsr.it (A. Tudda), ubeira.mariagiulia@hsr.it (M.G. Ubeira-Gabellini), broggi.sara@hsr.it (S. Broggi), jpascau@ing.uc3m.es (J. Pascau), lcubero@ing.uc3m.es (L. Cubero), cozzarini.cesare@hsr.it (C. Cozzarini), r.de-crevoisier@rennes.unicancer.fr (R. De Crevoisier), tiziana.rancati@istitutotumori.mi.it (T. Rancati), acosta@univ-rennes.fr (O. Acosta), fiorino.claudio@hsr.it (C. Fiorino).

https://doi.org/10.1016/j.phro.2023.100488
Received 13 April 2023; Received in revised form 22 August 2023; Accepted 23 August 2023
Available online 28 August 2023

A promising approach for reducing the risk of adverse symptoms is to identify sub-regions of the organ whose dose-volume metrics may be better associated to worsened symptoms. Evidence of correlations between local dose and side effects was provided by analyzing dose volume histograms (DVHs), i.e. graphical representations of the distribution of radiation dose delivered to different volumes of a specific anatomical structure or target within the patient's body. In this case, DVHs were assessed at sub-anatomical scales below the organ level [5]. As a clinically relevant example, several studies have highlighted the high sensitivity of the bladder trigone region, emphasizing the need for dose limitations in this specific area [6–9]. Expanding on this concept, dose-outcome correlations can be examined by analyzing the 3D dose distribution overall or within specific organs at risk (OARs).

Various methodologies have been developed to investigate the dose–effect relationship at the voxel level across a population to identify anatomical regions (symptom-related sub-regions, i.e. SRSs) that may contribute to the occurrence of toxicity events [5,10,11]. Previous studies have employed these techniques, including both 2D analyses based on surface maps and 3D analyses [8,9,12–25]. To the best of our knowledge, there have been limited studies focusing on adapting treatment plans to spare SRSs volumes [26,27]. To address this issue, advanced techniques such as Multi-Criteria Optimization (MCO) could be employed for the fine tuning of the dose distributions. According to the MCO approach [28–36], multiple spatial dose distributions will yield the same or similar DVHs for the relevant OARs, some of which could be sub-optimal. By identifying SRSs and reducing the dose locally without affecting the entire OAR DVHs, the risk of radio-induced toxicity can potentially be reduced.

The objective of this study was to investigate the feasibility of a customized dose optimization approach for SRSs, utilizing knowledge-based (KB) models for automatic treatment planning combined to MCO. The integration of this approach into an automated workflow aims to reduce inter-operator variability and facilitate the consideration of new optimization objectives, which may be hard to manage using a standard planning method.

2. Material and methods

2.1. Clinical protocol

Forty-five high-risk prostate cancer patients previously treated at San Raffaele Hospital (HSR) with Helical TomoTherapy (HTT) were selected. Patients were treated according to our moderately hypofractionated Institutional protocol, including pelvic node irradiation in a simultaneous integrated boost (SIB) approach. Details of contouring, margin definition, dose prescription and planning strategy may be found elsewhere [37,38]; in short, PTV_{high} (prescription dose of 74.2 Gy/28 fractions) included prostate and the proximal third of seminal vesicles (CTV_{high}), minus the overlap with the rectum (Overlap); the cranial portion of seminal vesicles (CTV_{int}) was considered as PTV_{int} (65.5 Gy); pelvic lymph nodes (CTV_{low}) were considered as PTV_{low} (51.8 Gy). The dose to the Overlap was constrained to 65.5 Gy. The current study was conducted under the project number 110 - JTC PerPlanRT ERA PerMed (GA 779282) and confirmed by the involved institutions.

2.2. Symptom-related sub-structure segmentation method

Mylona at Al. [19,20] and Dréan et al. [39] performed a voxel-wise analysis of the dose distribution in the rectum, urethra and bladder; a comparison between a with-toxicity and a without-toxicity cohort allowed the identification of six sub-regions predictive of: 3-year rectal bleeding (sub-rectal region, SRR); acute incontinence (INC_ACU); acute retention (RET_ACU); late retention (RET_LAT); late dysuria (DYS_LAT), late hematuria (HEM_LAT). Three sub-regions located in the urethra and bladder were successfully validated as more predictive of urinary toxicity than the whole bladder for urinary incontinence, retention, and dysuria [19].

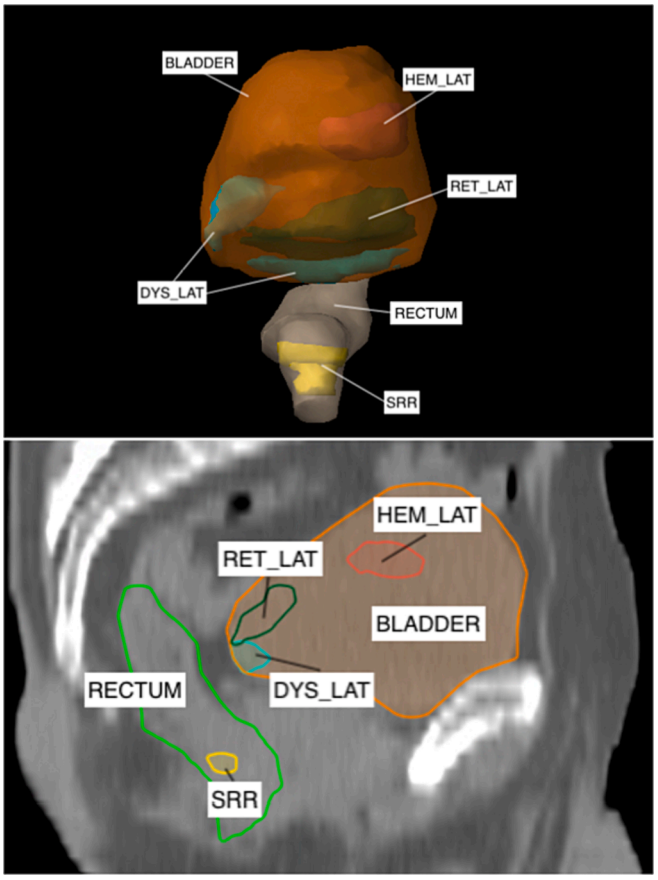

Fig. 1. Symptom related sub-regions (SRSs) position within bladder and rectum.

Contours of the urethral-vesical SRSs for the forty-five patient cohort were generated at Centre Eugène Marquis (University of Rennes), using deformable registration based on the structural description of the bladder, prostate and urethra [20,39–41]. Details can be found in the Supplementary materials. Given that the incontinence-related region is very small and almost completely overlaid on the PTV_{high}, it was not considered in this study.

Furthermore, the decision was made to analyze only late symptom regions. Therefore, the four examined regions were SRR, DYS_LAT, HEM_LAT and RET_LAT. Fig. 1 illustrates a representation of these SRSs and their positions within the bladder and rectum. Once the contours of the sub-structures were available, a preliminary analysis was performed on their volumes and the dose they received with the HTT treatment delivered in the clinic.

2.3. KB Plan

The KB approach involves developing predictive models for DVHs by modelling past information, specifically previously treated patient data. A training process aims to build a model which can be used to predict the optimal dose distribution for any new case (patient) with its own geometrical/anatomical specificity.

A model based on data for patients treated according to HSR Institutional protocol with HTT for high-risk prostate cancer patients was previously developed and validated, with details previously published [42]. For the present study, this model was selected to generate treatment plans that meet clinical standards for each of the forty-five patients, without taking into consideration the identified SRSs. These automatic plans (KB plans) served as a starting point to obtain further

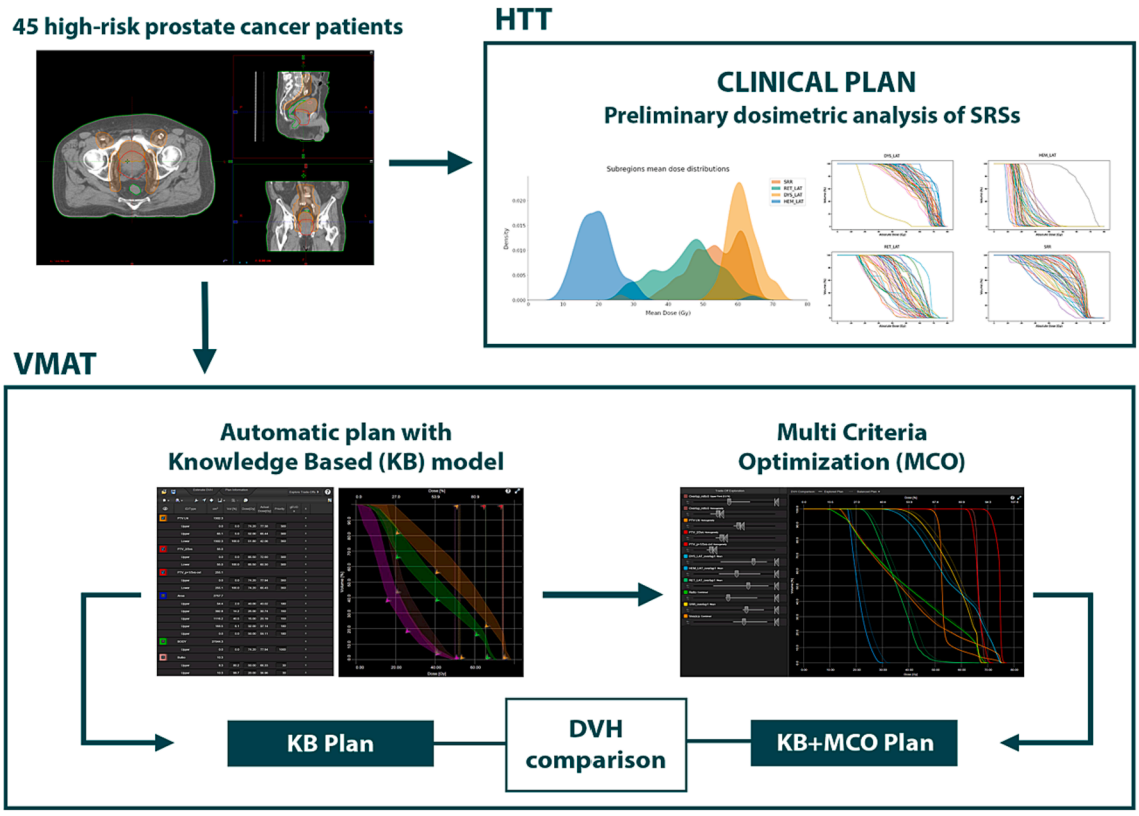

Fig. 2. Planning workflow. The HTT clinical plan was used to perform a preliminary dosimetric analysis of SRSs. Then, for each patient, a good quality plan was automatically created using a knowledge based previously trained model (KB plan). A further multi-criteria optimization (MCO) was performed using the trade-off exploration tool. Finally, differences between KB plan and KB + MCO plan were evaluated through a DVHs comparison.

optimized plans using MCO (KB + MCO plans). Minor modifications were required to adapt the KB-TOMO model to the VMAT modality due to the incompatibility between the available MCO module and the HTT system utilized at HSR. Details on the template modifications can be found in the Supplementary materials (Table S1).

The treatment equipment considered was a Varian DHX 6 MV X-rays Linac with 120-leaf Millennium MLC. Four complete VMAT arcs with collimator rotation of 15 degrees were used. A set of clinical goals was defined: for high, intermediate and low dose PTVs the minimum value of V95% was set to 95%. The final calculation of the plan was performed in the Eclipse environment (Eclipse, 16.1).

2.4. KB + MCO Plan

The trade-Off Exploration tool of Eclipse available in HSR radiotherapy research station (TBox Varian Eclipse, 16.1) allowed real-time exploration and visual assessment of the range of trade-offs in target coverage and preservation of healthy tissue. Once a previously optimized plan, i.e. the KB-plan, was available, structures and targets for the trade-off examination were chosen. A collection of optimized and representative plans was then generated and used to examine the compromises among optimization objectives. The plan database was examined using the selected objective sliders to find the best-compromised plan for the purpose. Defined clinical objectives were also used to limit the range of examination. DVHs, isodoses and clinical objectives values were examined to assess the impact of the trade-offs; a figure explaining the system functionality is available in the Supplementary material (Figure S1). Of note, an initial balanced plan influences the Pareto front generation and is therefore crucial for a successful exploration of the trade-off. In this study, each balanced plan was generated based on the HSR Institutional KB model, guaranteeing a clinically acceptable treatment plan as a starting point.

To reduce SRS mean doses without compromising PTV coverage/homogeneity or OARs sparing, the following trade-off objectives were selected: dose homogeneity for all the targets (PTV_{high}, PTV_{int}, PTV_{low}, Overlap); maximum dose for the Overlap; mean dose for bladder, rectum, DYS_LAT, HEM_LAT, RET_LAT and SRR. The following general criteria were adopted for the optimization: a) dose homogeneity for targets had to change as little as possible; b) DVHs of the whole rectum/bladder and other OARs (penile bulb, femoral heads and bowel cavity) should not have worsened; c) the mean dose of SRSs had to decrease as much as possible while respecting the previous criteria.

At this feasibility stage, the operator chose the best plan optimization, giving the same importance to all SRSs and trying to reduce the dose in the sub-structures as homogeneously as possible. Once the "best" plan was chosen, it could be converted into the corresponding deliverable one, and the dose distribution for this final KB + MCO plan could be calculated (See Fig. 2 summarizing the workflow of the study).

2.5. DVHs analysis

For each patient, DVHs resulting from KB and KB + MCO plans were computed for SRSs, OARs and PTVs, and compared. The examined OARs were bowel, bladder, rectum, penile bulb and femoral heads.

Mean changes were assessed: the difference between KB + MCO plan and KB plan was evaluated (ΔVolume [%]) for each absolute dose bin (with a 0.1 Gy step) for each of the structures considered. Dose intervals where the difference was statistically significant were identified by the Wilcoxon non-parametric test between the two DVHs. For the structures under consideration, selected dose-volume parameters were extracted, specifically: mean dose, D1% (taken as the maximum dose), V95%, V20Gy, V40Gy, V60Gy, V70Gy. Differences between KB and KB + MCO plan were evaluated for these parameters and statistically significant differences were assessed with the Wilcoxon test.

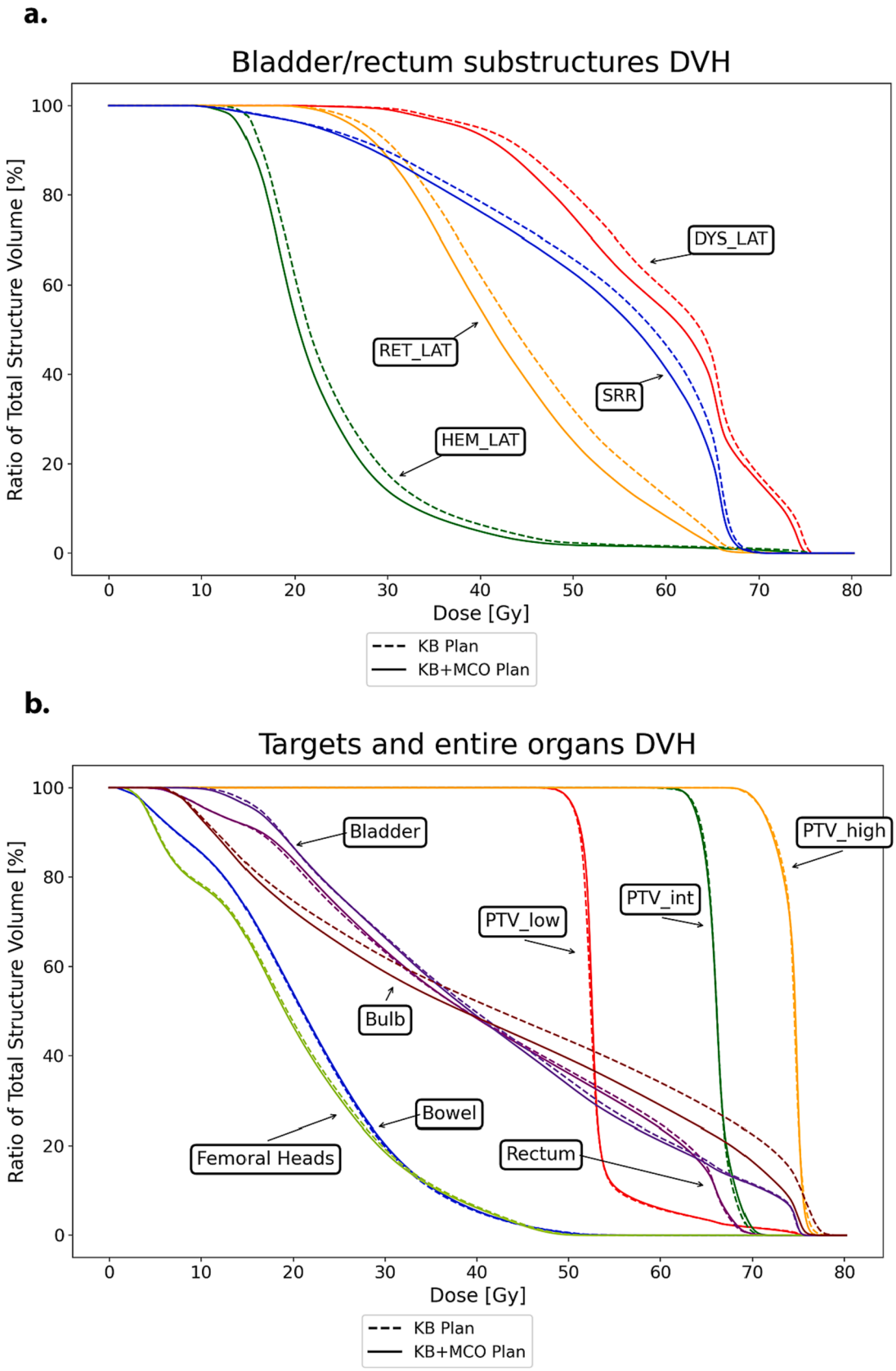

Fig. 3. Mean DVHs of the KB (dashed lines) and KB + MCO plan (continuous lines) relating to bladder and rectum sub-structures (a) and targets and entire OARs (b).

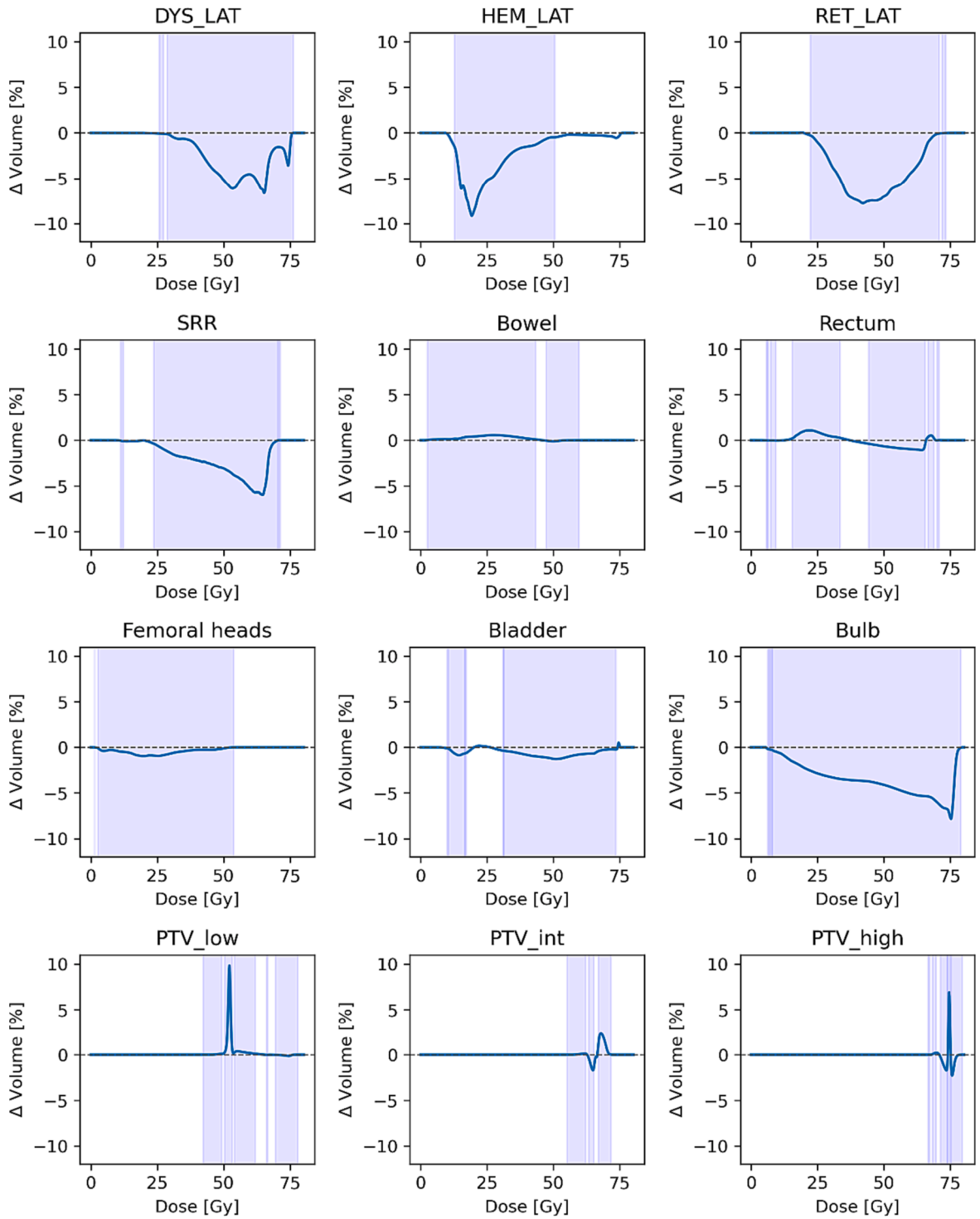

Fig. 4. Average differences between the DVHs of the two plans (KB + MCO plan minus KB plan) for SRSs, OARs and targets. Dose ranges corresponding to statistically significant differences are filled in light blue (p-value < 0.05). (For interpretation of the references to colour in this figure legend, the reader is referred to the web version of this article.)

Furthermore, differences in Monitor Units between the KB and KB + MCO plans were assessed as an indicator of treatment plan complexity. For each of the four VMAT arcs, the KB plan MU value was subtracted from the KB + MCO plan MU value.

3. Results

3.1. Dose to SRSs without intervention: Clinical plan data

Mean value of the bladder volume across the forty-five patients was 279 ± 157 cm^3, 79 ± 22 cm^3 for the rectum. Mean volume of SRS ranged from 5 ± 2 cm^3 for SRR to 12 ± 4 cm^3 for DYS_LAT (Supplementary materials, Table S2 and Figure S2). Figure S3 in Supplementary

Table 1
Selected dose-volume parameters were extracted: mean dose, D1%, V95%, V20Gy, V40Gy, V60Gy, V70Gy. The data includes both median values and ranges. Statistically significant differences between KB and KB + MCO plan were assessed with Wilcoxon test. P-values < 0.05 are marked in bold.

Structure	Features	KB PLAN		KB+MCO PLAN		ΔKB+MCO-KB		p-value
		Median	Range	Median	Range	Median	Range	
PTV_low	Mean Dose [Gy]	53.3	[52.8 ; 54.5]	53.5	[53.0 ; 54.7]	0.1	[-0.4 ; 0.5]	**≪0.01**
	D1% [Gy]	72.4	[66.6 ; 75.5]	72.1	[66.2 ; 75.3]	-0.4	[-1.2 ; 0.0]	**≪0.01**
	V95% [%]	99.0	[98.2 ; 99.6]	99.1	[98.1 ; 99.6]	0.2	[-0.3 ; 0.7]	**0.02**
PTV_int	Mean Dose [Gy]	66.2	[65.4 ; 66.7]	66.2	[65.5 ; 66.8]	0.1	[-0.4 ; 0.6]	0.4
	D1% [Gy]	69.8	[69.0 ; 70.6]	70.2	[69.4 ; 71.0]	0.4	[-0.2 ; 1.1]	**≪0.01**
	V95% [%]	99.6	[96.9 ; 100.0]	99.7	[96.1 ; 100.0]	0.1	[-2.1 ; 1.4]	**≪0.01**
PTV_high	Mean Dose [Gy]	74.2	[74.2 ; 74.2]	74.2	[73.6 ; 74.2]	0.0	[-0.6 ; 0.0]	**≪0.01**
	D1% [Gy]	76.7	[75.8 ; 77.5]	76.3	[75.6 ; 77.0]	-0.5	[-1.5 ; 0.2]	**≪0.01**
	V95% [%]	96.7	[94.7 ; 98.8]	96.7	[94.9 ; 98.3]	0.0	[-1.3 ; 2.6]	0.1
Overlap	Mean Dose [Gy]	66.5	[66.0 ; 69.7]	66.5	[66.0 ; 69.5]	0.0	[-0.6 ; 0.4]	0.9
	D1% [Gy]	69.4	[68.2 ; 71.5]	69.4	[68.2 ; 71.6]	0.0	[-0.9 ; 0.7]	0.8
	V95% [%]	99.9	[99.0 ; 100.0]	99.9	[98.9 ; 100.0]	0.0	[-0.1 ; 0.4]	**≪0.01**
DYS_LAT	Mean Dose [Gy]	60.4	[36.1 ; 71.7]	58.5	[34.8 ; 70.5]	-1.3	[-3.5 ; -0.1]	**≪0.01**
	D1% [Gy]	73.2	[51.6 ; 75.8]	73.2	[51.4 ; 75.3]	-0.4	[-3.6 ; 0.5]	**≪0.01**
	V40gy [%]	99.5	[17.6 ; 100]	97.8	[14.8 ; 100]	-0.5	[-9.8 ; 0.5]	**≪0.01**
	V60gy [%]	60.6	[0.0 ; 99.6]	55.1	[0.0 ; 96.7]	-3.7	[-20.3 ; 0.2]	**≪0.01**
	V70gy [%]	7.5	[0.0 ; 76.0]	7.4	[0.0 ; 68.6]	-0.8	[-9.6 ; 4.5]	**≪0.01**
HEM_LAT	Mean Dose [Gy]	22.2	[15.4 ; 65.0]	20.7	[12.4 ; 61.2]	-1.3	[-4.3 ; 0.6]	**≪0.01**
	D1% [Gy]	32.9	[18.6 ; 75.6]	29.8	[17.2 ; 74.0]	-2.5	[-8.1 ; -0.5]	**≪0.01**
	V20gy [%]	67.2	[0.0 ; 100.0]	54.8	[0.0 ; 100.0]	-6.1	[-48.3 ; 8.8]	**≪0.01**
	V40gy [%]	0.0	[0.0 ; 97.0]	0.0	[0.0 ; 92.9]	0.0	[-15.4 ; 0.0]	**≪0.01**
	V60gy [%]	0.0	[0.0 ; 72.4]	0.0	[0.0 ; 62.6]	0.0	[-9.7 ; 0.0]	**≪0.01**
	V70gy [%]	0.0	[0.0 ; 45.5]	0.0	[0.0 ; 31.1]	0.0	[-14.4 ; 0.0]	**≪0.01**
RET_LAT	Mean Dose [Gy]	45.6	[32.4 ; 59.8]	42.8	[30.9 ; 56.1]	-2.2	[-5.1 ; 0.3]	**≪0.01**
	D1% [Gy]	64.9	[44.4 ; 72.6]	62.8	[41.4 ; 72.3]	-2.8	[-7.3 ; 0.2]	**≪0.01**
	V40gy [%]	100.0	[93.4 ; 100.0]	100.0	[96.8 ; 100.0]	-6.1	[-29.5 ; 1.8]	**≪0.01**
	V60gy [%]	63.2	[14.9 ; 100.0]	54.3	[4.0 ; 100.0]	-2.0	[-32.8 ; 0.0]	**≪0.01**
	V70gy [%]	9.4	[0.0 ; 58.5]	3.3	[0.0 ; 46.0]	0.0	[-2.1 ; 0.1]	**≪0.01**
SRR	Mean Dose [Gy]	54.5	[35.5 ; 65.0]	53.6	[34.2 ; 64.2]	-1.4	[-2.8 ; 0.2]	**≪0.01**
	D1% [Gy]	67.6	[59.5 ; 70.6]	67.3	[57.8 ; 70.6]	-0.5	[-2.3 ; 0.7]	**≪0.01**
	V20gy [%]	100.0	[73.3 ; 100]	100.0	[72.0 ; 100.0]	0.0	[-2.2 ; 1.5]	**≪0.01**
	V40gy [%]	81.4	[32.0 ; 100.0]	81.9	[29.1 ; 100.0]	-1.4	[-8.9 ; 1.1]	**≪0.01**
	V60gy [%]	45.8	[0.7 ; 97.4]	39.2	[0.2 ; 85.7]	-3.8	[-24.0 ; 0.0]	**≪0.01**
Rectum	Mean Dose [Gy]	40.9	[31.1 ; 46.4]	41.2	[30.6 ; 46.5]	0.0	[-2.7 ; 1.4]	1.0
	D1% [Gy]	68.6	[67.8 ; 71.2]	68.7	[67.6 ; 71.3]	0.2	[-0.7 ; 1.0]	**0.02**
	V20gy [%]	83.0	[69.5 ; 91.5]	84.2	[68.5 ; 93.3]	0.9	[-1.0 ; 3.6]	**≪0.01**
	V40gy [%]	50.1	[24.8 ; 63.2]	50.1	[23.9 ; 63.7]	0.1	[-9.2 ; 3.0]	0.8
	V60gy [%]	25.6	[11.5 ; 35.2]	24.5	[10.6 ; 34.2]	-0.9	[-6.2 ; 0.4]	**≪0.01**
Bladder	Mean Dose [Gy]	42.6	[32.5 ; 54.0]	41.7	[31.1 ; 54.6]	-0.3	[-1.6 ; 0.6]	**≪0.01**
	D1% [Gy]	75.0	[74.3 ; 75.5]	75.1	[74.6 ; 75.5]	0.1	[-0.4 ; 0.5]	0.07
	V20gy [%]	87.1	[66.7 ; 99.9]	87.4	[63.4 ; 100.0]	-0.3	[-3.7 ; 5.4]	0.6
	V40gy [%]	49.0	[30.0 ; 75.2]	48.2	[27.8 ; 76.7]	-0.6	[-4.7 ; 1.2]	**≪0.01**
	V60gy [%]	21.5	[9.7 ; 46.8]	21.1	[8.8 ; 47.5]	-0.7	[-2.2 ; 0.7]	**≪0.01**
	V70gy [%]	10.6	[4.6 ; 29.6]	10.5	[4.3 ; 30.1]	-0.1	[-1.2 ; 0.6]	**≪0.01**
Bowel	Mean Dose [Gy]	21.6	[10.0 ; 27.7]	21.9	[10.0 ; 27.9]	0.1	[-0.6 ; 0.4]	**≪0.01**
	D1% [Gy]	47.4	[37.6 ; 52.1]	47.3	[38.4 ; 52]	-0.3	[-1.7 ; 0.8]	**≪0.01**
	V20gy [%]	53.3	[22.0 ; 79.5]	53.2	[22.2 ; 80.1]	0.4	[-2.0 ; 1.8]	**≪0.01**
	V40gy [%]	4.5	[0.5 ; 13.0]	4.7	[0.4 ; 13.6]	0.2	[-1.7 ; 1.1]	**≪0.01**
Femoral heads	Mean Dose [Gy]	20.3	[16.9 ; 24.3]	19.8	[16.8 ; 24.1]	-0.2	[-1.4 ; 0.2]	**≪0.01**
	D1% [Gy]	46.5	[42.6 ; 51]	45.9	[41.3 ; 50.1]	-0.6	[-2.0 ; 1.3]	**≪0.01**
	V20gy [%]	46.8	[27.8 ; 67.4]	45.6	[26.4 ; 66.7]	-0.7	[-7.7 ; 1.5]	**≪0.01**
	V40gy [%]	6.1	[2.1 ; 12.2]	6.1	[1.7 ; 12.0]	-0.3	[-1.6 ; 1.0]	**≪0.01**
Bulb	Mean Dose [Gy]	44.7	[13.7 ; 71.0]	41	[13.8 ; 69.4]	-2.7	[-7.3 ; 0.6]	**≪0.01**
	D1% [Gy]	76.8	[31.0 ; 78.7]	75.3	[32.1 ; 77.3]	-1.9	[-10.8 ; 1.1]	**≪0.01**
	V20gy [%]	79.8	[13.7 ; 100.0]	76.2	[14.6 ; 100.0]	-0.7	[-8.3 ; 2.9]	**≪0.01**
	V40gy [%]	53.5	[0.0 ; 99.8]	47.9	[0.0 ; 99.7]	-3.3	[-15.2 ; 1.6]	**≪0.01**
	V60gy [%]	33.9	[0.0 ; 89.8]	27.0	[0.0 ; 87.8]	-5.1	[-14.4 ; 0.0]	**≪0.01**
	V70gy [%]	21.2	[0.0 ; 71.3]	13.1	[0.0 ; 64.5]	-6.7	[-18.3 ; 0.0]	**≪0.01**

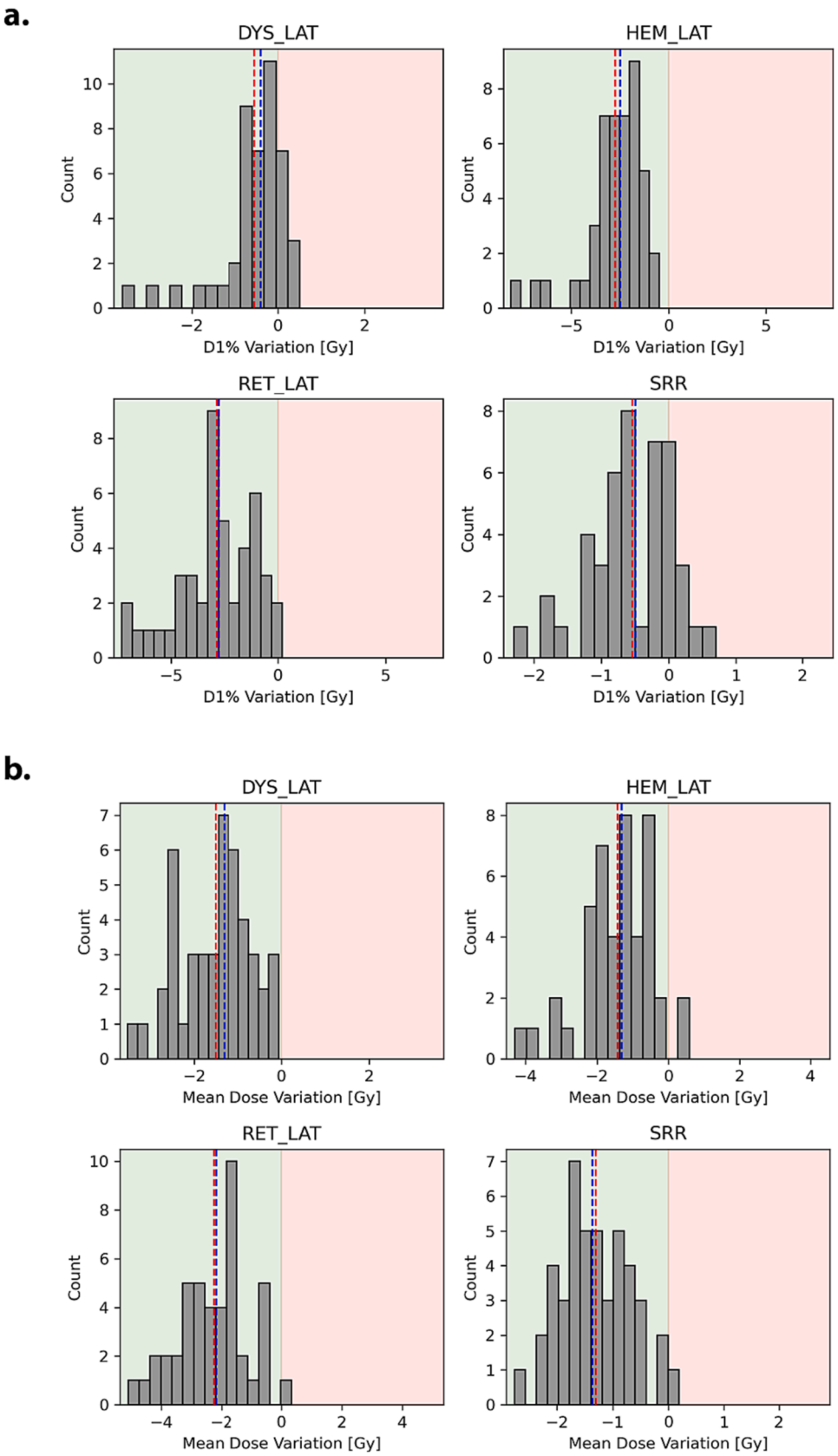

Fig. 5. Distribution of mean dose (a) and D1% (b) differences between KB + MCO and KB plan among the forty-five patients, for the four SRSs. Blue and red lines show the median and mean values, respectively. (For interpretation of the references to colour in this figure legend, the reader is referred to the web version of this article.)

materials indicates notable variations in DVHs of SRS derived from clinical plan dose distributions, reflecting patient-specific differences primarily driven by the extent of SRS-PTV overlap. Similar variability was observed in maximum and mean doses for all four SRSs, as depicted in Figure S4 and Table S3.

3.2. Comparison between KB and KB + MCO plan

The transition from KB to KB + MCO plan resulted in dose reduction across all four SRSs (Fig. 3a). Notably, OAR DVHs remained nearly identical for both plans, with a remarkable decrease observed for the penile bulb. Similarly, the three targets displayed minimal changes, characterized by a slight elevation in the high-dose tail for PTV_{int} in the KB + MCO plan (Fig. 4). Consistently with the observations in section 3.1, this case also demonstrated patient-specific variability (Supplementary materials, Figure S5).

An average decrease was evident in both mean dose and D1% to SRSs across the forty-five patients (Table 1). Notably, exceptions of significance emerged for D1% in DYS_LAT and SRR. Although the average variation remained below zero, a marginal (<1 Gy) increase in D1% was discernible in a minority of patients (Fig. 5, Figure S6, Figure S7). The median difference in Monitor Units between the KB and KB + MCO plans was −0.4 MU, with a range spanning from −31.4 to 34.8 MU.

4. Discussion

A combination of KB approach and MCO was proposed and investigated for optimizing prostate cancer radiotherapy with VMAT. It was demonstrated that this method allows for selective sparing of the bladder and rectum's considered SRSs without detrimental effects on PTVs coverage and overall OARs sparing, compared to the KB automatic plan. The complexity of the treatment plan, evaluated in terms of number of monitor units, remained unchanged.

Selective sparing of the SRR was also recently discussed by Lafond et al [26], reporting a significant reduction in mean dose for the rectum and SRR compared to clinical plans (3.6 and 7.7 Gy respectively). In our study, four sub-structures were simultaneously spared, resulting in a mean dose reduction between 1.3 and 2.2 Gy, with a maximum reduction up to 3–5 Gy. As there is a clear interplay between the sparing of one SRS with respect to the others, our results concerning the rectal SRR may be considered quite consistent with those of Lafond et al. While the proposed workflow's effectiveness has been demonstrated, it is important to introduce optimization criteria that consider specific dose–effect relationships for each SRS. The criteria implicitly adopted at this feasibility stage were not based on quantitative risk assessment.

Additionally, the clinical significance of each SRS is an issue: for example, the location of HEM_LAT could simply be a result of field propagation on a template in a large population of patients, each with a different bladder volume and filling level. The selective sparing of this region, quite distant from the high-dose PTV, may not be as crucial as for DYS_LAT and RET_LAT, which are situated near the vesical neck and trigone. Several studies suggest a significant role of the trigone in the development of urinary toxicity [3,7–9,22], indicating it as a more sensitive region within the bladder. Furthermore, the DYS_LAT region was identified and confirmed using different methods in two independent cohorts [19]. On the other hand, the selective sparing of the rectal SRR may also be justified by the observed dose-area effect for the absolute rectum area irradiated [18]. A steeper drop of the dose in that region could better preserve a larger portion of the rectal wall and reduce the likelihood of rectal bleeding, as reported in several pixel-wise analyses based on rectal dose-surface maps [13,17,21,43,44]. However, the clinical meaning of the association between the DVH of SRR and rectal bleeding remains questionable, as it may be interpreted as a surrogate of the impact of the overlap between the anterior rectum and the PTV resulting from voxel-wise analysis. Voxel-wise analyses have limitations and depend on the dose and spatial features of the specific investigated cohort. The findings do not imply causality but are rather dependent on the dose distribution. The availability of large cohorts with diverse dose distribution patterns (for instance variable margins, prescribed doses, strategies in handling rectum-PTV overlap) could lead to the identification of more clinically interpretable sub-regions.

Once dose–effect relationships are established, the relative importance of sparing each SRS can be considered, and MCO can be performed using the corresponding gEUD (generalized Equivalent Uniform Dose), which incorporates the radiobiological response of the sub-regions and the corresponding NTCP [45,46]. This refined approach is currently under investigation within the PerPlanRT project, under which the current study was conducted (Era-learn website [47]). Additionally, the dose per fraction may play an important role in determining the likelihood of adverse outcomes, especially for the bladder, which has shown unexpected sensitivity to fractionation in postprostatectomy [48–50] and radically treated patients [51–53]. Recent estimates of α/β ratio for dysuria, incontinence and hematuria endpoints suggest that the therapeutic gain for GU toxicity through hypofractionation could be lower than expected, emphasizing the importance of selectively sparing sensitive SRSs in hypofractionated protocols [49–51].

Although the identified sub-structures may not have all immediate clinical interpretation, it is worth noting that alternative dose distributions with improved OARs sparing were achieved without compromising target coverage compared to the solution found by the KB model alone. The potential inclusion of MCO in a fully automatic workflow could prove beneficial and enhance the capabilities of automatic planning models.

CRediT authorship contribution statement

Lisa Alborghetti: Methodology, Software, Validation, Formal analysis, Investigation, Writing – original draft. **Roberta Castriconi:** Conceptualization, Methodology, Investigation, Writing – original draft. **Carlos Sosa Marrero:** Methodology, Software, Resources, Writing – review & editing. **Alessia Tudda:** Investigation, Methodology, Software, Validation, Formal analysis, Investigation, Writing – original draft. **Maria Giulia Ubeira-Gabellini:** Software, Investigation, Writing – review & editing. **Sara Broggi:** Writing – review & editing. **Javier Pascau:** Methodology, Software, Resources, Writing – review & editing. **Lucia Cubero:** Resources, Writing – review & editing. **Cesare Cozzarini:** Conceptualization, Methodology, Investigation, Writing – original draft. **Renaud De Crevoisier:** Conceptualization, Methodology, Resources, Writing – review & editing. **Tiziana Rancati:** Conceptualization, Methodology, Resources, Writing – review & editing. **Oscar Acosta:** Conceptualization, Methodology, Investigation, Resources, Writing – review & editing, Funding acquisition. **Claudio Fiorino:** Conceptualization, Methodology, Investigation, Writing – original draft, Writing – review & editing, Supervision.

Declaration of Competing Interest

The authors declare that they have no known competing financial interests or personal relationships that could have appeared to influence the work reported in this paper.

Acknowledgments

This work has been supported by Fondazione Regionale per la Ricerca Biomedica, project nr. 110 - JTC PerPlanRT ERA PerMed, GA 779282. Frank Bagg is acknowledged for the linguistic revision.

Appendix A. Supplementary data

Supplementary data to this article can be found online at https://doi.org/10.1016/j.phro.2023.100488.

References

[1] Rancati T, Fiorino C. Modelling radiotherapy side effects: Practical applications for planning optimisation. CRC press; 2019.

[2] Rancati T, Palorini F, Cozzarini C, Fiorino C, Valdagni R. Understanding urinary toxicity after radiotherapy for prostate cancer: first steps forward. Tumori 2017; 103:395–404. https://doi.org/10.5301/tj.5000681.

[3] Landoni V, Fiorino C, Cozzarini C, Sanguineti G, Valdagni R, Rancati T. Predicting toxicity in radiotherapy for prostate cancer. Phys Med 2016;32:521–32. https://doi.org/10.1016/j.ejmp.2016.03.003.

[4] Bentzen SM. Radiation dose-response relationships. Basic Clin. Radiobiol. fifth, CRC press; 2018.

[5] Ebert MA, Gulliford S, Acosta O, De Crevoisier R, McNutt T, Heemsbergen WD, et al. Spatial descriptions of radiotherapy dose: normal tissue complication models and statistical associations. Phys Med Biol 2021:66. https://doi.org/10.1088/1361-6560/ac0681.

[6] Ghadjar P, Zelefsky MJ, Spratt DE, Munck af Rosenschöld P, Oh JH, Hunt M, et al. Impact of dose to the bladder trigone on long-term urinary function after high-dose intensity modulated radiation therapy for localized prostate cancer. Int J Radiat Oncol Biol Phys 2014;88:339–44. 10.1016/j.ijrobp.2013.10.042.

[7] Heemsbergen WD, Al-Mamgani A, Witte MG, van Herk M, Pos FJ, Lebesque JV. Urinary obstruction in prostate cancer patients from the Dutch trial (68 Gy vs. 78 Gy): relationships with local dose, acute effects, and baseline characteristics. Int J Radiat Oncol Biol Phys 2010;78:19–25. https://doi.org/10.1016/j.ijrobp.2009.07.1680.

[8] Improta I, Palorini F, Cozzarini C, Rancati T, Avuzzi B, Franco P, et al. Bladder spatial-dose descriptors correlate with acute urinary toxicity after radiation therapy for prostate cancer. Phys Med 2016;32:1681–9. https://doi.org/10.1016/j.ejmp.2016.08.013.

[9] Palorini F, Cozzarini C, Gianolini S, Botti A, Carillo V, Iotti C, et al. First application of a pixel-wise analysis on bladder dose-surface maps in prostate cancer radiotherapy. Radiother Oncol 2016;119:123–8. https://doi.org/10.1016/j.radonc.2016.02.025.

[10] Acosta O, De Crevoisier R. Beyond DVH: 2D/3D-Based Dose Comparison to Assess Predictors of Toxicity. Model. Radiother. Side Eff., CRC Press; 2019.

[11] Rigaud B, Simon A, Castelli J, Lafond C, Acosta O, Haigron P, et al. Deformable image registration for radiation therapy: principle, methods, applications and evaluation. Acta Oncol 2019;58:1225–37. https://doi.org/10.1080/0284186X.2019.1620331.

[12] Acosta O, Drean G, Ospina JD, Simon A, Haigron P, Lafond C, et al. Voxel-based population analysis for correlating local dose and rectal toxicity in prostate cancer radiotherapy. Phys Med Biol 2013;58:2581–95. https://doi.org/10.1088/0031-9155/58/8/2581.

[13] Buettner F, Gulliford SL, Webb S, Partridge M. Modeling late rectal toxicities based on a parameterized representation of the 3D dose distribution. Phys Med Biol 2011; 56:2103–18. https://doi.org/10.1088/0031-9155/56/7/013.

[14] Buettner F, Gulliford SL, Webb S, Sydes MR, Dearnaley DP, Partridge M. Assessing correlations between the spatial distribution of the dose to the rectal wall and late rectal toxicity after prostate radiotherapy: an analysis of data from the MRC RT01 trial (ISRCTN 47772397). Phys Med Biol 2009;54:6535–48. https://doi.org/10.1088/0031-9155/54/21/006.

[15] Dréan G, Acosta O, Lafond C, Simon A, de Crevoisier R, Haigron P. Interindividual registration and dose mapping for voxelwise population analysis of rectal toxicity in prostate cancer radiotherapy. Med Phys 2016;43:2721–30. https://doi.org/10.1118/1.4948501.

[16] Hoogeman MS, van Herk M, de Bois J, Muller-Timmermans P, Koper PCM, Lebesque JV. Quantification of local rectal wall displacements by virtual rectum unfolding. Radiother Oncol 2004;70:21–30. https://doi.org/10.1016/j.radonc.2003.11.015.

[17] Marcello M, Denham JW, Kennedy A, Haworth A, Steigler A, Greer PB, et al. Increased Dose to Organs in Urinary Tract Associates With Measures of Genitourinary Toxicity in Pooled Voxel-Based Analysis of 3 Randomized Phase III Trials. Front Oncol 2020;10:1174. https://doi.org/10.3389/fonc.2020.01174.

[18] Munbodh R, Jackson A, Bauer J, Schmidtlein CR, Zelefsky MJ. Dosimetric and anatomic indicators of late rectal toxicity after high-dose intensity modulated radiation therapy for prostate cancer. Med Phys 2008;35:2137–50. https://doi.org/10.1118/1.2907707.

[19] Mylona E, Ebert M, Kennedy A, Joseph D, Denham J, Steigler A, et al. Rectal and Urethro-Vesical Subregions for Toxicity Prediction After Prostate Cancer Radiation Therapy: Validation of Voxel-Based Models in an Independent Population. Int J Radiat Oncol Biol Phys 2020;108:1189–95. https://doi.org/10.1016/j.ijrobp.2020.07.019.

[20] Mylona E, Cicchetti A, Rancati T, Palorini F, Fiorino C, Supiot S, et al. Local dose analysis to predict acute and late urinary toxicities after prostate cancer radiotherapy: Assessment of cohort and method effects. Radiother Oncol 2020;147: 40–9. https://doi.org/10.1016/j.radonc.2020.02.028.

[21] Onjukka E, Fiorino C, Cicchetti A, Palorini F, Improta I, Gagliardi G, et al. Patterns in ano-rectal dose maps and the risk of late toxicity after prostate IMRT. Acta Oncol 2019;58:1757–64. https://doi.org/10.1080/0284186X.2019.1635267.

[22] Yahya N, Ebert MA, House MJ, Kennedy A, Matthews J, Joseph DJ, et al. Modeling Urinary Dysfunction After External Beam Radiation Therapy of the Prostate Using Bladder Dose-Surface Maps: Evidence of Spatially Variable Response of the Bladder Surface. Int J Radiat Oncol Biol Phys 2017;97:420–6. https://doi.org/10.1016/j.ijrobp.2016.10.024.

[23] McWilliam A, Dootson C, Graham L, Banfill K, Abravan A, Van Herk M. Dose surface maps of the heart can identify regions associated with worse survival for lung cancer patients treated with radiotherapy. Phys Imaging Radiat Oncol 2020; 15:46–51. https://doi.org/10.1016/j.phro.2020.07.002.

[24] Shelley LEA, Sutcliffe MPF, Thomas SJ, Noble DJ, Romanchikova M, Harrison K, et al. Associations between voxel-level accumulated dose and rectal toxicity in prostate radiotherapy. Phys Imaging Radiat Oncol 2020;14:87–94. https://doi.org/10.1016/j.phro.2020.05.006.

[25] Casares-Magaz O, Moiseenko V, Witte M, Rancati T, Muren LP. Towards spatial representations of dose distributions to predict risk of normal tissue morbidity after radiotherapy. Phys Imaging Radiat Oncol 2020;15:105–7. https://doi.org/10.1016/j.phro.2020.08.002.

[26] Lafond C, Barateau A, N'Guessan J, Perichon N, Delaby N, Simon A, et al. Planning With Patient-Specific Rectal Sub-Region Constraints Decreases Probability of Toxicity in Prostate Cancer Radiotherapy. Front Oncol 2020;10:1597. https://doi.org/10.3389/fonc.2020.01597.

[27] Monti S, Palma G, D'Avino V, Gerardi M, Marvaso G, Ciardo D, et al. Voxel-based analysis unveils regional dose differences associated with radiation-induced morbidity in head and neck cancer patients. Sci Rep 2017;7:7220. https://doi.org/10.1038/s41598-017-07586-x.

[28] Buschmann M, Seppenwoolde Y, Wiezorek T, Weibert K, Georg D. Advanced optimization methods for whole pelvic and local prostate external beam therapy. Phys Med 2016;32:465–73. https://doi.org/10.1016/j.ejmp.2016.03.002.

[29] Cagni E, Botti A, Chendi A, Iori M, Spezi E. Use of knowledge based DVH predictions to enhance automated re-planning strategies in head and neck adaptive radiotherapy. Phys Med Biol 2021:66(13). https://doi.org/10.1088/1361-6560/ac08b0.

[30] Craft D, McQuaid D, Wala J, Chen W, Salari E, Bortfeld T. Multicriteria VMAT optimization: Multicriteria VMAT optimization. Med Phys 2012;39:686–96. https://doi.org/10.1118/1.3675601.

[31] Ehrgott, M. Multicriteria Optimization. Springer Science & Business Media; 2005.

[32] Miguel-Chumacero E, Currie G, Johnston A, Currie S. Effectiveness of Multi-Criteria Optimization-based Trade-Off exploration in combination with RapidPlan for head & neck radiotherapy planning. Radiat Oncol 2018;13:229. https://doi.org/10.1186/s13014-018-1175-y.

[33] Müller BS, Shih HA, Efstathiou JA, Bortfeld T, Craft D. Multicriteria plan optimization in the hands of physicians: a pilot study in prostate cancer and brain tumors. Radiat Oncol 2017;12:168. https://doi.org/10.1186/s13014-017-0903-z.

[34] Teichert K, Currie G, Küfer K-H, Miguel-Chumacero E, Süss P, Walczak M, et al. Targeted multi-criteria optimisation in IMRT planning supplemented by knowledge based model creation. Oper Res Health Care 2019;23:100185. https://doi.org/10.1016/j.orhc.2019.04.003.

[35] Wala J, Craft D, Paly J, Zietman A, Efstathiou J. Maximizing dosimetric benefits of IMRT in the treatment of localized prostate cancer through multicriteria optimization planning. Med Dosim 2013;38:298–303. https://doi.org/10.1016/j.meddos.2013.02.012.

[36] Wang J, Chen Z, Li W, Qian W, Wang X, Hu W. A new strategy for volumetric-modulated arc therapy planning using AutoPlanning based multicriteria optimization for nasopharyngeal carcinoma. Radiat Oncol 2018;13:94. https://doi.org/10.1186/s13014-018-1042-x.

[37] Di Muzio N, Fiorino C, Cozzarini C, Alongi F, Broggi S, Mangili P, et al. Phase I-II study of hypofractionated simultaneous integrated boost with tomotherapy for prostate cancer. Int J Radiat Oncol Biol Phys 2009;74:392–8. https://doi.org/10.1016/j.ijrobp.2008.08.038.

[38] Di Muzio NG, Fodor A, Noris Chiorda B, Broggi S, Mangili P, Valdagni R, et al. Moderate Hypofractionation with Simultaneous Integrated Boost in Prostate Cancer: Long-term Results of a Phase I-II Study. Clin Oncol 2016;28:490–500. https://doi.org/10.1016/j.clon.2016.02.005.

[39] Dréan G, Acosta O, Ospina JD, Fargeas A, Lafond C, Corrégé G, et al. Identification of a rectal subregion highly predictive of rectal bleeding in prostate cancer IMRT. Radiother Oncol 2016;119:388–97. https://doi.org/10.1016/j.radonc.2016.04.023.

[40] Cubero L, García-Elcano L, Mylona E, Boue-Rafle A, Cozzarini C, Giulia Ubeira Gabellini M, et al. Deep Learning-based Segmentation of Prostatic Urethra on Computed Tomography Scans for Treatment Planning. Phys Imaging. Radiat Oncol 2023;26(100431). https://doi.org/10.1016/j.phro.2023.100431.

[41] Klein S, Staring M, Murphy K, Viergever MA, Pluim J. elastix: A Toolbox for Intensity-Based Medical Image Registration. IEEE Trans Med Imaging 2010;29: 196–205. https://doi.org/10.1109/TMI.2009.2035616.

[42] Castriconi R, Cattaneo GM, Mangili P, Esposito P, Broggi S, Cozzarini C, et al. Clinical Implementation of Knowledge-Based Automatic Plan Optimization for Helical Tomotherapy. Pract Radiat Oncol 2021;11:e236–44. https://doi.org/10.1016/j.prro.2020.09.012.

[43] Casares-Magaz O, Muren LP, Moiseenko V, Petersen SE, Pettersson NJ, Høyer M, et al. Spatial rectal dose/volume metrics predict patient-reported gastro-intestinal symptoms after radiotherapy for prostate cancer. Acta Oncol 2017;56:1507–13. https://doi.org/10.1080/0284186X.2017.1370130.

[44] Heemsbergen WD, Incrocci L, Pos FJ, Heijmen BJM, Witte MG. Local Dose Effects for Late Gastrointestinal Toxicity After Hypofractionated and Conventionally Fractionated Modern Radiotherapy for Prostate Cancer in the HYPRO Trial. Front Oncol 2020;10:469. https://doi.org/10.3389/fonc.2020.00469.

[45] Fogliata A, Thompson S, Stravato A, Tomatis S, Scorsetti M, Cozzi L. On the gEUD biological optimization objective for organs at risk in Photon Optimizer of Eclipse treatment planning system. J Appl Clin Med Phys 2018;19:106–14. https://doi.org/10.1002/acm2.12224.

[46] Niemierko A. Reporting and analyzing dose distributions: a concept of equivalent uniform dose. Med Phys 1997;24:103–10. https://doi.org/10.1118/1.598063.

[47] Era-learn website: https://www.era-learn.eu/network-information/networks/era-permed/multidisciplinary-research-projects-on-personalised-medicine-2013-pre-clinical-research-big-data-and-ict-implementation-and-user2019s-perspective/personalized-planning-in-radiotherapy-through-integrative-modeling-of-local-dose-effect-and-new-dosimetric-constraints.

[48] Bresolin A, Garibaldi E, Faiella A, Cante D, Vavassori V, Waskiewicz JM, et al. Predictors of 2-Year Incidence of Patient-Reported Urinary Incontinence After Post-prostatectomy Radiotherapy: Evidence of Dose and Fractionation Effects. Front Oncol 2020;10:1207. https://doi.org/10.3389/fonc.2020.01207.

[49] Cozzarini C, Fiorino C, Deantoni C, Briganti A, Fodor A, La Macchia M, et al. Higher-than-expected severe (Grade 3–4) late urinary toxicity after postprostatectomy hypofractionated radiotherapy: a single-institution analysis of 1176 patients. Eur Urol 2014;66:1024–30. https://doi.org/10.1016/j.eururo.2014.06.012.

[50] Fiorino C, Cozzarini C, Rancati T, Briganti A, Cattaneo GM, Mangili P, et al. Modelling the impact of fractionation on late urinary toxicity after postprostatectomy radiation therapy. Int J Radiat Oncol Biol Phys 2014;90:1250–7. https://doi.org/10.1016/j.ijrobp.2014.08.347.

[51] Brand DH, Brüningk SC, Wilkins A, Naismith O, Gao A, Syndikus I, et al. The Fraction Size Sensitivity of Late Genitourinary Toxicity: Analysis of Alpha/Beta (α/β) Ratios in the CHHiP Trial. Int J Radiat Oncol Biol Phys 2023;115:327–36. https://doi.org/10.1016/j.ijrobp.2022.08.030.

[52] Cozzarini C, Rancati T, Palorini F, Avuzzi B, Garibaldi E, Balestrini D, et al. Patient-reported urinary incontinence after radiotherapy for prostate cancer: Quantifying the dose-effect. Radiother Oncol 2017;125:101–6. https://doi.org/10.1016/j.radonc.2017.07.029.

[53] Sanguineti G, Arcidiacono F, Landoni V, Saracino BM, Farneti A, Arcangeli S, et al. Macroscopic Hematuria After Conventional or Hypofractionated Radiation Therapy: Results From a Prospective Phase 3 Study. Int J Radiat Oncol Biol Phys 2016;96:304–12. https://doi.org/10.1016/j.ijrobp.2016.05.017.